Published online 15 May 2013 *Nucleic Acids Research, 2013, Vol. 41, No. 13* **6501–6513**
doi:10.1093/nar/gkt397

The helicase FBH1 is tightly regulated by PCNA via CRL4(Cdt2)-mediated proteolysis in human cells

Agathe Bacquin[1,2], Caroline Pouvelle[1,2], Nicolas Siaud[1], Mylène Perderiset[3,4], Sophie Salomé-Desnoulez[5], Carine Tellier-Lebegue[6], Bernard Lopez[1], Jean-Baptiste Charbonnier[6] and Patricia L. Kannouche[1,2,*]

[1]Université Paris-Sud, CNRS-UMR8200 Unit of Genetic Stability and Oncogenesis, Institut de cancérologie Gustave Roussy, Villejuif, France, [2]Equipe labellisée Ligue Contre le Cancer, Institut de cancérologie Gustave Roussy, Villejuif, France, [3]Telomeres and Cancer laboratory; Institut Curie, 26 rue d'Ulm, 75248 Paris, France, [4]UPMC Univ. Paris 6, F-75005 Paris, France, [5]Plate-forme Imagerie et Cytométrie, IRCIV -Institut de cancérologie Gustave Roussy, Villejuif, France and [6]Laboratory of Structural Biology and Radiobiology, Commissariat à l'Energie Atomique et aux Energies Alternatives, Institut de Biologie et de Technologies de Saclay, 91191 Gif-s-Yvette, France

Received November 11, 2012; Revised April 15, 2013; Accepted April 18, 2013

ABSTRACT

During replication, DNA damage can challenge replication fork progression and cell viability. Homologous Recombination (HR) and Translesion Synthesis (TLS) pathways appear as major players involved in the resumption and completion of DNA replication. How both pathways are coordinated in human cells to maintain genome stability is unclear. Numerous helicases are involved in HR regulation. Among them, the helicase FBH1 accumulates at sites of DNA damage and potentially constrains HR *via* its anti-recombinase activity. However, little is known about its regulation *in vivo*. Here, we report a mechanism that controls the degradation of FBH1 after DNA damage. Firstly, we found that the sliding clamp Proliferating Cell Nuclear Antigen (PCNA) is critical for FBH1 recruitment to replication factories or DNA damage sites. We then showed the anti-recombinase activity of FBH1 is partially dependent on its interaction with PCNA. Intriguingly, after its re-localization, FBH1 is targeted for degradation by the Cullin-ring ligase 4-Cdt2 ($CRL4^{Cdt2}$)–PCNA pathway *via* a PCNA-interacting peptide (PIP) degron. Importantly, expression of non-degradable FBH1 mutant impairs the recruitment of the TLS polymerase eta to chromatin in UV-irradiated cells. Thus, we propose that after DNA damage, FBH1 might be required to restrict HR and then degraded by the Cdt2–proteasome pathway to facilitate TLS pathway.

INTRODUCTION

In eukaryotes, Homologous Recombination (HR) mechanism plays a key role in repair of various DNA damages including double-strand breaks (DSB), DNA gaps, stalled or collapsed replication forks (1). By contrast, inappropriate recombination events can cause genomic instability by inducing unscheduled genome rearrangements and/or accumulation of toxic recombination intermediates. Several helicases have been described to play a critical role in HR regulation (2). Among them, Srs2 limits recombination events in *Saccharomyces cerevisiae* by dismantling the Rad51 nucleofilament (3,4). Recently, the human F-box DNA helicase FBH1 has been proposed to act as a functional homologue of Srs2 in human cells by sharing its anti-recombinase activity (5,6). Similar to Srs2, FBH1 belongs to the UvrD family of helicases and contains also an F-box, which makes it able to form a Skp1–Cul1–F-box (SCF) ubiquitin ligase complex (5,7). Genetic studies in *S. cerevisiae* show that FBH1 partially compensate for the loss of Srs2 and orthologues of FBH1 in *Schizosaccharomyces pombe* and chicken DT40 cells would limit Rad51-mediated recombination at replication fork (5,8,9). In human, FBH1 accumulates as nuclear foci at sites of DNA damage and replication stress. Its knockdown leads to elevated numbers of Rad51 foci in S phase, and an increase in the rate of sister chromatid exchange (SCE) whereas its over-expression impairs Rad51 recruitment and reduces the level of I-SceI-induced HR (6). Taken together, these observations lead to the idea that FBH1 has an anti-recombinogenic activity, which has to be tightly controlled to maintain genome integrity. However, the regulation of the helicase FBH1 in human cells is unknown.

*To whom correspondence should be addressed. Tel: +33 1 42 11 40 30; Fax: +33 1 42 11 50 08; Email: patricia.kannouche@igr.fr

In *S. cerevisiae*, Srs2 is recruited at replication forks by direct interaction with the SUMOylated form of the Proliferating Cell Nuclear Antigen (PCNA) to perform its anti-recombinase function (10–12). The homotrimeric ring PCNA plays a major role in coordinating DNA replication, DNA repair and damage tolerance pathways. It mediates the recruitment of various proteins involved in the DNA damage response (13). Among them, translesion polymerase η (Polη) is recruited by the mono-ubiquinated form of PCNA at stalled replication forks to bypass UV-induced DNA lesions (14,15).

Interaction between PCNA and its partners is most often mediated by the PCNA-interacting peptide (PIP)-box. Recently, a novel motif termed AlkB homologue 2 PCNA-interacting motif (APIM) was found in a number of proteins interacting with PCNA including hABH2, Rad51B and hTFIIS-L (16,17).

PCNA was also proposed to stimulate the degradation of several proteins. Indeed, following UV irradiation, as well as in S phase of the cell cycle, the E3 ubiquitin ligase Cullin-ring ligase 4-Cdt2 ($CRL4^{Cdt2}$) promotes the ubiquitination and the degradation of numerous proteins including Cdt1, p21 or Set8 to prevent genomic instability [for review, see (18)]. Importantly, this destruction is dependent on their binding to PCNA through a specialized PIP-box named PIP degron. Therefore, it appears that PCNA is not only at the crossroad of multiple pathways but can also regulate the levels of key proteins in human cells.

Here, we addressed the question of FBH1 regulation in human cells by examining its spatiotemporal dynamics during DNA replication and after UV irradiation. We report that FBH1 recruitment to replication factories or to sites of DNA damage is mediated by PCNA, through its PIP and APIM motifs. Importantly, we show that FBH1 stability is greatly decreased after DNA damage. We demonstrate that FBH1 is ubiquitinated and degraded in a PCNA- Cdt2- and PIP degron-dependent manner. Finally, we show that FBH1 degradation is critical for Pol η proper recruitment at stalled replication forks.

MATERIALS AND METHODS

Cell culture and treatments

Human MRC5-V1 (named MRC5 in the text) cells were grown in Minimal Eagle Medium (MEM; Gibco) supplemented with 10% fetal calf serum (FCS), 100 U/ml penicillin and 100 μg/ml streptomycin under 5% CO_2. The generation of subline RG37, containing a single chromosomally integrated copy of the recombination reporter plasmid pDR-GFP, was described previously (19). HeLa, RG37 and HEK 293 T cells were grown in D-MEM (Dulbecco's Modified Eagle medium) containing sodium pyruvate, penicillin/streptomycin and 10% FCS. Global and local UV-C irradiations were performed as described before (20). Cycloheximide and MG132 purchased from Sigma were used at 25 μg/ml and 10 μM, respectively.

Antibodies and immunological techniques

For immunoprecipitation, HEK 293T cells were harvested in PBS and lysed in Lysis Buffer [50 mM Tris (pH 7.5), 20 mM NaCl, 1 mM $MgCl_2$, 0.1% SDS, protease inhibitor cocktail (Roche) and 50 U/ml benzonase (novagen)]. Cell lysates were then incubated overnight (o/n) with indicated antibodies. Protein A-sepharose beads were then added for 1 h 30 min before washing and heating–denaturation. Proteins were separated by electrophoresis in 8% SDS-PAGE gels and analysed by western blotting. Antibodies used for western blotting and immunofluorescence were purchased from Abcam (Cdt2, Fen1, GAPDH, GFP, Polη), Santa-Cruz (FBH1, lamin A/C, PCNA), Bethyl (Cdt1, DDB1), Sigma (γ-tubulin, β-actin), BD Biosciences (β-catenin), Covance (HA-11) and Rockland (Cul4A). Antibodies used for immunoprecipitation were purchased from Santa-Cruz (HA F-7) and DakoCytomation (negative control mouse IgG2a).

HR assay

RG37 cells were co-transfected with 100 ng of HA-tagged-I-SceI expression vector and 1 μg of transgene [empty vector, phCMV2 (Gene Therapy Systems) or HA-FBH1]. Transfections were carried out using JetPEI (Polyplus) according to manufacturer's protocol. Cells were collected 48 h after transfection by trypsinization, and recombinant cells were measured by flow cytometry analysis. The efficiency of co-transfection was followed by western blotting using an anti-HA antibody.

HR assay after siRNA transfection

RG37 cells were transfected with 20 μM of non-targeting siRNA or siRNA against FBH1 (ON-TARGETplus SMARTpool, Dharmacon) using INTERFERin reagent (Polyplus). Twenty-four hours later, cells were co-transfected with 250 ng of HA-tagged-I-SceI expression vector and 1 μg of transgene using JetPEI (Polyplus). Recombinant cells were measured by flow cytometry analysis 72 h after siRNAs transfection.

His pull-down and cell fractionation

To perform His pull-down, HEK 293T cells were lysed in denaturing conditions (100 mM NaH_2PO_4, 10 mM Tris-Cl, 8 M urea, 20 mM Imidazole, pH 8), centrifuged and supernatant was incubated with Ni-NTA-agarose (Qiagen) for 1 h at 4°C before washing and heating denaturation. Cell fractionation was performed as previously described (21).

Immunofluorescence and videomicroscopy analysis

For immunofluorescence analysis, cells grown on coverslips were rinsed twice with cold PBS and fixed with 4% paraformaldehyde with 0.2% Triton X-100 for 25 min, then permeabilized with 0.5% Triton X-100 in PBS for 15 min, and blocked in PBS with 3% Bovine Serum Albumin (BSA) and 0.05% Tween 20, for 30 min at RT. Immunodetection of proteins was performed by incubating the cells with indicated primary antibodies, o/n at 4°C. After washes, coverslips were then incubated with Alexa Fluor 488 (green) or 594 (red) anti-mouse or anti-rabbit secondary antibodies (Invitrogen) for 45 min at

RT then mounted with Dako Faramount Aqueous Mounting Medium (Dako) containing DAPI.

For videomicroscopy analysis, cells were plated in 35 mm dishes (Ibidi), transfected with indicated plasmids, and treated with HaloTag TMR Direct Ligand (Promega) according to manufacturer's protocol. Cells were then imaged using Fluoview FV10i-W confocal microscope (Olympus), at 37°C under 5% CO_2.

Plasmid construction, siRNA sequences and cell transfection

GFP-Polη construct has been previously described (20). peGFP-PCNA was constructed by digesting the previously described vectors pCMV2-HA-PCNA (21) with XhoI and BamHI and inserted into the XhoI-BamHI sites of the peGFP-C3 vector (BD Biosciences). Halo-tagged PCNA and His-tagged ubiquitin were gifts from C. Gelot and S. Aoufouchi (Institut Gustave Roussy, France). To generate eGFP-FBH1wt and HA-FBH1wt, FBH1 cDNA was amplified by PCR from pCR4-TOPO-FBH1 (clone n°8322429, Open Biosystems) using the forward primer 5′-ctcgtcgacgatatcATGAGAC GGTTTAAGCGGAAGCATCTT-3′ and the reverse primer 5′-actggtaccTCAGAAGACGAGGAAGAGCAG GGCCTCAT-3′. The PCR product was digested with SalI and KpnI, and inserted into the vector peGFP-C3 (BD Biosciences) or phCMV2 (Gene Therapy Systems) by cloning into restriction sites XhoI and KpnI. pCDNA-FBH1wt was constructed by digesting phCMV2-FBH1 with EcoRV and KpnI and cloning into restriction sites EcoRV and KpnI of pcDNA3.1/Zeo(−) (Invitrogen). For generating FBH1 mutants, site-directed mutagenesis (QuickChange II site-directed mutagenesis kit, Stratagene) was carried out using FBH1 wt constructs as template according to the manufacturer's protocol to introduce the following mutations: [Q61A, I64A, F67A, F68A] (mut PIP), [K807A, F808A, I809A] (mut APIM), [Q61A, I64A, E66A, F67A, F68A, K72A] (mut PIPdeg6A), [P65A, E66A, K72A] (mut PIPdeg3A), [K72A] (mut PIPdegK + 4A).

siRNAs were purchased from Eurogentec: non-targeting siRNA [SR-CL000-005], siRNA PCNA [GCC GAGAUCUCAGCCAUAU], siRNA Cul4A [GAACU UCCGAGACAGACCU], siRNA Cul4B [AAGCCUA AAUUACCAGAAA] and Dharmacon: DDB1 [ON-TARGETplus SMARTpool], FBXO18 [ON-TARGETplus SMARTpool], Cdt2 [ON-TARGETplus SMARTpool] and siRNA Cdt2 [GCGCUUGAAUAGA GGCUUA].

Transient transfection was performed using Exgen500 (Fermentas) according to the manufacturer's protocol, and cells were analysed 24 h later. For stable transfection, cells were transfected using FuGENE 6 (Roche), and stable phCMV2-HA-FBH1 transfectants were isolated and further propagated in medium containing 0.6 mg/ml geneticin (Gibco). Halo-PCNA stable population kindly provided by J. Cebrian (IGR, France) was propagated in medium containing 1 μg/ml blasticidine. siRNAs transfection was performed using INTER FERin reagent (Polyplus), and cells were analysed 72 h later.

PCNA purification, PIP and APIM peptides preparation and isothermal titration calorimetry

PCNA purification was performed as described previously (22). The synthetic peptides FBH1 PIP and APIM, and ABH2 APIM peptides were purchased from Genecust at 95% purity, and the concentrations of the stock peptide solutions were determined by amino acid composition.

Binding between PCNA and the different peptides was determined by isothermal titration calorimetry (ITC) using a VP-ITC calorimeter (GE-Healthcare). Prior to measurements, all solutions were degassed under vacuum. The reaction cell was loaded with 20–130 μM PCNA solution. Control experiments were performed with peptide solutions injected into buffer. Thermodynamic parameters ΔH, N, and Ka were obtained by non-linear least-squares fitting of the experimental data using the single set of independent binding sites model of the Origin software provided with the instrument. The free energy of binding (ΔG) and the entropy (ΔS) were determined using the classical thermodynamic formulas: $\Delta G = -RT \ln(Ka)$ and $\Delta G = \Delta H - T\Delta S$. All binding experiments were performed at 6°C in 20 mM Tris buffer, pH 7.5, containing 10 mM β-mercaptoethanol. Competition experiments were realized by titrating PCNA by calorimetry with 2-fold excess of p21 PIP and injecting APIM motif of FBH1.

RESULTS

PCNA recruits FBH1 to sites of DNA replication and DNA damage *via* a classical PIP-box and an APIM motif

It has been reported that FBH1 accumulated into discrete nuclear foci after exposure of cells to ionizing radiation (IR) or hydroxyurea (HU) (6). To investigate further the regulation of the subcellular localization of FBH1, we examined its distribution in normally cycling cells or following UV irradiation. In absence of exogenous DNA damage, FBH1 is uniformly distributed in the nucleoplasm in most cells (Figure 1A). However, 20–25% of cells displayed FBH1 foci, which colocalized with the DNA sliding clamp PCNA known to form replication foci in S-phase. To visualize cells in S-phase, fibroblasts were incubated with the nucleoside analogue 5-ethynyl-2′-deoxyuridine (EdU). Using click chemistry, we found that most cells displaying FBH1 foci were also EdU positive (Figure 1A). These results indicate that FBH1 accumulates at sites of DNA replication during the S-phase of unperturbed cells. In addition, in response to local UV irradiation, FBH1 is able to accumulate at sites of DNA damage within 1 h where it co-localizes with PCNA and persists at least 3 h (Figure 1B). This cellular distribution was also observed by expressing untagged or GFP-tagged FBH1 demonstrating that this localization is specific to the helicase and not of the tag used (data not shown).

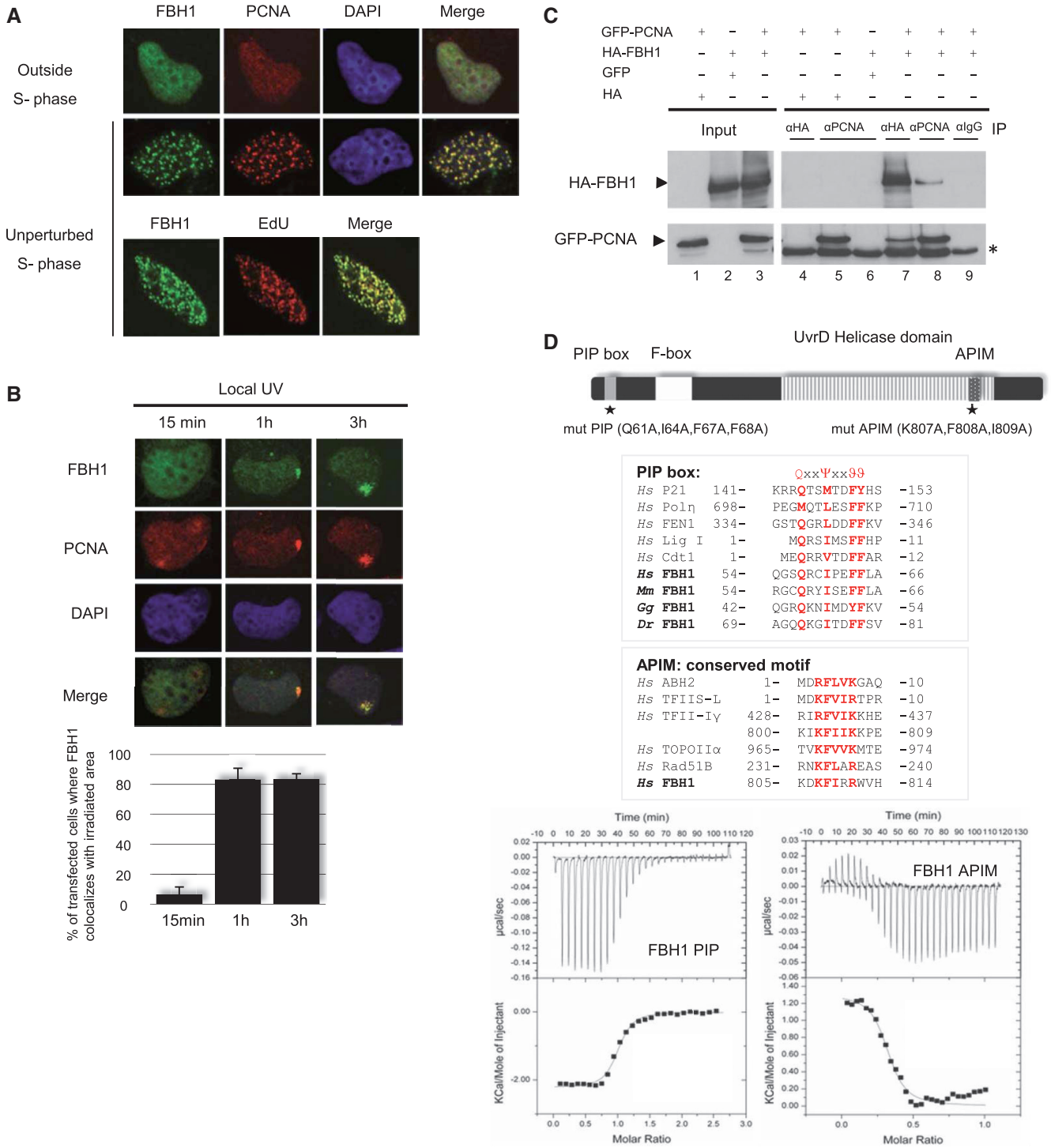

Figure 1. FBH1 interacts with PCNA via two distinct motifs, PIP-box and APIM. (**A**) MRC5 cells expressing ectopic FBH1 were fixed and co-stained for FBH1 (green) and PCNA (red) or EdU (red). DNA is visualized in blue. Representative images are shown for each condition. (**B**) MRC5 cells expressing HA-FBH1 were locally UV irradiated at 100 J/m2 and co-stained for FBH1 (green), PCNA (red) and DNA (blue) at indicated time. Representative images are shown. Each image represents >600 FBH1-positive cells in three independent experiments. The graph shows the percentage of green cells displaying HA-FBH1 accumulation to local irradiation area. Mean of three independent experiments (± SD). (**C**) Immunoprecipitation against HA-tag or PCNA was performed from extracts of 293T cells co-expressing HA-FBH1 and GFP-PCNA and analysed by western-blotting. Asterisk denoted aspecific signal. (**D**) Schematic of FBH1 protein with its PIP-box and APIM motif. Punctual mutations used for functional study are shown (top panel). Sequence alignment of the PIP-box and APIM motif of known proteins. Canonical residues are shown in red (middle panel). Thermogram and binding isotherm of titration of FBH1 PIP box wt (right) and APIM wt (left) peptides into PCNA solution were assessed by ITC at 6°C (bottom panel).

PCNA is known to play a key role in DNA replication and DNA repair by forming a sliding homotrimeric ring around DNA that serves as a docking platform for the recruitment of various DNA-modifying enzymes including DNA polymerases, helicases and nucleases (13). We then tested whether the helicase FBH1 is able to interact with PCNA *in vivo*. We co-expressed HA-FBH1 and GFP-PCNA in 293T and performed immunoprecipitation experiments. The function of tagged PCNA has previously been assessed and does not significantly differ from untagged PCNA (14,21). We observed that FBH1 co-immunoprecipitated with PCNA and reciprocally (Figure 1C, Lane 7–8).

The *in silico* analysis of FBH1 amino acid sequence revealed two putative PCNA-binding motifs: a PCNA-interacting peptide known as PIP-box with the consensus sequence Q-X-X-(I/L/M)-X-X-(F/Y)-(F/Y) at the N-terminus, and a more recently described PCNA-binding motif called APIM (AlkB homologue 2 PCNA-interacting motif) with the consensus sequence (K/R)-(F/Y/W)-(L/I/V/A)-(L/I/V/A)-(K/R) (16), at the C-terminus (Figure 1D, top and middle panels). To test the functionality of these motifs, we characterized by microcalorimetry the affinity and stoichiometry of the interaction between purified PCNA and synthetic peptides containing the PIP-box or APIM sequences (Figure 1D, bottom panel, left and right graphs respectively). We also examined the interaction between PCNA and the originally described APIM, i.e. ABH2 (Supplementary Figure S1A). The binding reaction between each peptide and PCNA gave an exothermic heat exchange fitting a one-site binding model after integration. The dissociation constant (Kd) of FBH1 PIP, FBH1 APIM and ABH2 APIM are 0.25 μM, 0.59 μM and 0.32 μM, respectively, at 6°C (Table 1). The mutation of PIP (FF to AA) or APIM (KFI to AAA) motifs abolished the binding to PCNA (Supplementary Figure S1B and C, and Table 1). These results demonstrated the ability of both APIM and PIP-box to mediate direct interaction between PCNA and FBH1.

To determine whether the interaction with PCNA is required to accumulate FBH1 at DNA damage sites or during S-phase, FBH1 mutants were generated in which the PIP and APIM motifs were individually or simultaneously altered (mut PIP, mut APIM and mut PIP + APIM, respectively). We found that in response to UV irradiation, the accumulation of single mutant of FBH1 on PIP or APIM (mut PIP, mut APIM) was impaired and completely abolished for the double mutant (mut PIP + APIM) (Figure 2A and B). Similar results were obtained for FBH1 accumulation to replication foci (Supplementary Figure S1E and F).

The FBH1 anti-recombinogenic activity partially depends on its interaction with PCNA

As it was previously shown that exogenous FBH1 impairs HR (6), we wondered whether PCNA-dependent recruitment of FBH1 was required for its anti-recombinogenic activity. To address this, we used a fibroblastic cell line bearing an integrated homologous recombination reporter composed of two differentially mutated GFP genes oriented as direct repeats. In this assay, HR is measured as the ability of cells to repair an I-SceI-induced double-strand break in the inactive GFP construct, which becomes functional only through HR-mediated repair, the control condition. The expression of the functional GFP was assessed by flow cytometry. Co-transfection of I-SceI-expressing plasmid with an empty HA vector served as reference for the maximal HR efficiency. We obtained 2.6% of GFP-positive cells, and this control condition was arbitrary fixed to 100% of HR efficiency. In agreement with previous study, exogenous HA-FBH1wt strongly decreased HR efficiency (14.4% versus 100%). Interestingly, the mutation of both PCNA interaction motifs PIP and APIM partially restores this efficiency (39.9%) whereas each of the single mutants has moderate or no effect on HR frequency (Figure 2C). The ratio between I-SceI and HA-FBH1 expression levels was similar for the different FBH1 constructs, suggesting that the differences in transfection efficiencies do not explain the differential effects of FBH1 mutants on HR efficiency (Figure 2D). To get closer to endogenous FBH1 levels, FBH1 overexpression was reduced by siRNA knock-down; non-targeting siRNA (siNT) was used as control (Supplementary Figure S1G and H). As reference for the maximal HR efficiency, we co-transfected I-SceI-expressing plasmid with an empty HA vector 24 h after transfection with siNT or siFBH1. In these control conditions, 4.7 and 3.9% of GFP-positive cells were

Table 1. Thermodynamic parameters obtained for the different PIP-box and APIM containing peptides

Peptide	Sequence	K_a (10^6 M)	K_d (μM)	ΔH° (kcal/mol)	−TΔS° (kcal/mol)	ΔG° (kcal/mol)
FBH1 PIP	$_{52}$RGQGS**Q**RC**I**P**EFF**LAGKQPCTN	3.9 ± 0.6	0.25 ± 0.3	−2.2 ± 0.1	−9.2 ± 0.3	−8.4 ± 0.1
FBH1 PIP (FF/AA)	$_{52}$RGQGS**Q**RC**I**P*AA*LAGKQPCTN	NI	NI	NI	NI	NI
FBH1 APIM	$_{605}$K**KFIRR**WVHKEGFSG	1.7 ± 0.5	0.59 ± 0.14	1.3 ± 0.1	−6.2 ± 0.2	−7.9 ± 0.1
FBH1 APIM (KFI/AAA)	$_{605}$K*AAA*R**R**WVHKEGFSG	NI	NI	NI	NI	NI
ABH2 APIM	$_{1}$M**DRFLVK**GAQGGLLRK	3.1 ± 1.0	0.32 ± 0.08	−1.2 ± 0.1	−7.0 ± 0.2	−8.3 ± 0.2
FBH1 PIPdeg6A	$_{52}$RGQGS*A*RC*A*P*AAA*LAG*A*QPCTN	NI	NI	NI	NI	NI
FBH1 PIPdeg3A	$_{52}$RGQGS**Q**RC**I***AA***FF**LAG*A*QPCTN	0.12 ± 0.03	8.7 ± 2.2	+1,7 ± 0.5	−8.2 ± 0.2	−6.5 ± 0.2
FBH1 PIPdegK + 4A	$_{52}$RGQGS**Q**RC**I**P**EFF**LAG*A*QPCTN	0.64 ± 0.05	1.6 ± 0.2	−3.3 ± 0.4	−4.1 ± 0.2	−7.4 ± 0.1

Numbers before peptide sequences correspond to the position in the protein sequence of the first amino acid of the peptide. The canonical positions of the PIP and APIM motifs are in bold characters and positions substituted for other amino acids are in italic. All experiments in this study were realized at 6°C to optimize the quality of the isothermal titration curves. NI means no interaction and indicates weak and constant signal under the condition used.

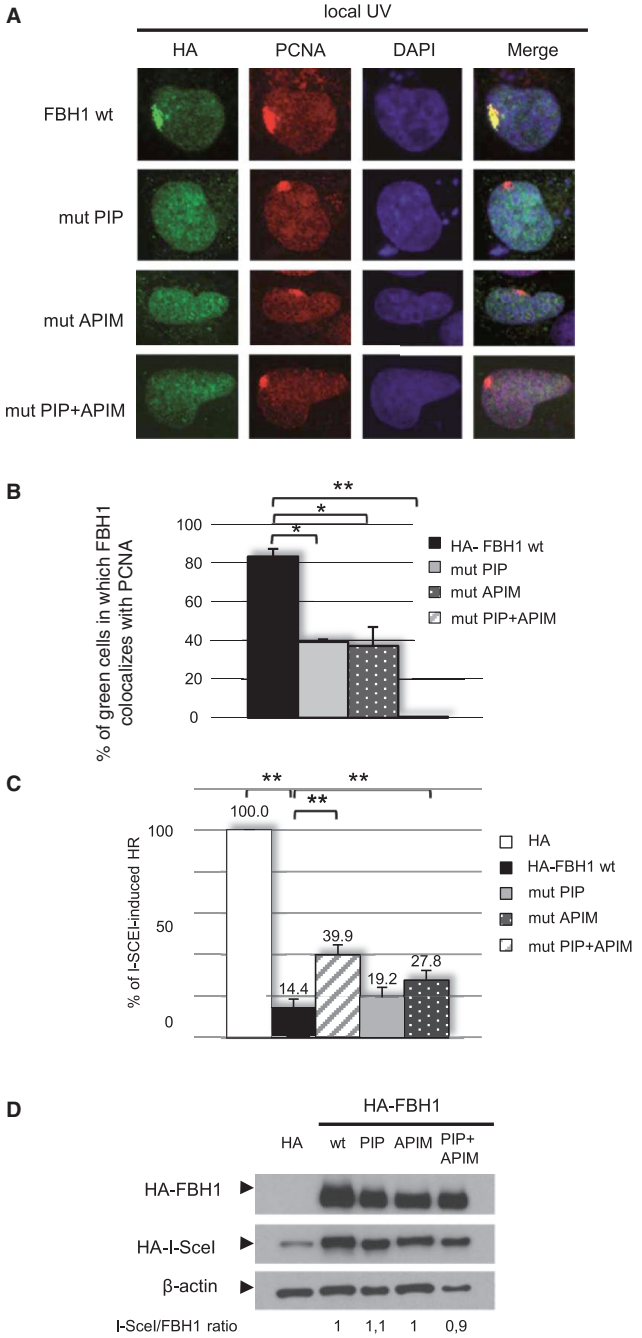

Figure 2. The PIP-box and APIM motif are required for FBH1 recruitment to sites of DNA damage and partially for its anti-recombinogenic activity. (**A** and **B**) MRC5 expressing HA-FBH1 wt or indicated mutants were locally irradiated at 100 J/m^2 then co-stained for HA (green), PCNA (red) and DNA (blue) 3 h later. The graph shows the percentage of green cells in which FBH1 co-localizes with PCNA. Mean of three independent experiments (±SD), $*P < 0.05$ and $**P < 0.005$ by Student's *t*-test. (**C** and **D**) The effects of exogenous HA-FBH1wt and indicated mutants on recombination induced by I-SceI were measured in RG37 cells as the amount of GFP-positive cells by flow cytometry analysis, in comparison with control cells expressing the empty vector. The values correspond to the mean percentage of HR efficiency, the control condition being arbitrary fixed to 100%. Mean of four independent experiments (±SD), $**P < 0.005$ by Student's *t*-test. In parallel, the levels of exogenous FBH1 and I-Sce1 were estimated by western blot using anti-HA antibody.

quantified respectively and arbitrary fixed to 100% of HR efficiency. Although the inhibitory effect of HA-FBH1 wt on HR was reduced after its knock-down, HR efficiency is still decreased (74.5%), and this decrease fully depends on the interaction between FBH1 and PCNA through both PIP and APIM motifs (106.4%), suggesting that when FBH1 is moderately overexpressed, its interaction with PCNA is indispensable for its anti-recombinogenic function. Collectively, these results demonstrate that PCNA mediates FBH1 recruitment to replication foci and UV-induced DNA damage through direct interaction via the PIP and APIM motifs and none of two is dispensable. Furthermore, the anti-recombinogenic role of FBH1 partially depends on its interaction with PCNA.

Proteasome-mediated degradation of FBH1 is enhanced after UV irradiation

To further investigate the spatiotemporal dynamics of FBH1 after UV damage and during replication, we performed confocal videomicroscopy on individual living cells expressing Halo-tagged PCNA and GFP-tagged FBH1. Cells were either mock treated or locally irradiated with UV, and imaged at fixed intervals. As expected, FBH1 recruitment to irradiated sites became visible within 1 h post-UV and reached highest foci intensity at about 1 h 30 min after treatment (Figure 3A, Supplementary Figure S2A and Supplementary Movies S1 and S2). Afterward, FBH1 levels progressively decreased and became barely visible 5 h post-UV while PCNA staining remained rather constant (Figure 3A). Similarly, in normally cycling cells, recruitment of FBH1 at sites of DNA replication is followed by a drastic decrease of FBH1 levels in comparison with non S phase cells (Figure 3B, Supplementary Figure S2B and C and Supplementary Movies S3 and S4). Because replicating and non-replicating cells were imaged by using the same exposure time, we can rule out photobleaching as cause of diminution of GFP-FBH1 fluorescence (Supplementary Figure S2A–C). These results strongly suggested a temporal regulation of FBH1 that could be mediated by degradation.

We then measured the half-life of ectopic HA-FBH1 in untreated cells and found that protein levels went down within 1 h, dropping to one-tenth 5 h after cycloheximide (chx) treatment. In contrast, addition of the proteasome inhibitor MG132 restored FBH1 stability (Figure 2C). The half-life of untagged ectopic FBH1 was similar (Supplementary Figure S2D), demonstrating that this degradation is not due to the HA tag. Moreover, incubation of cells with MG132 alone leads to the accumulation of slower migrating forms of FBH1 (Figure 3D), which seem to be poly-ubiquitin chains. Altogether, these results suggest that the decrease of FBH1 levels in cells is due to its degradation by the proteasome after poly-ubiquitination.

We reasoned that the protein levels of transiently overexpressed FBH1 is highly superior to endogenous FBH1 and could be overtaken by the proteasome to maintain protein levels close to the endogenous level. We then explored the regulation of endogenous FBH1 in HeLa

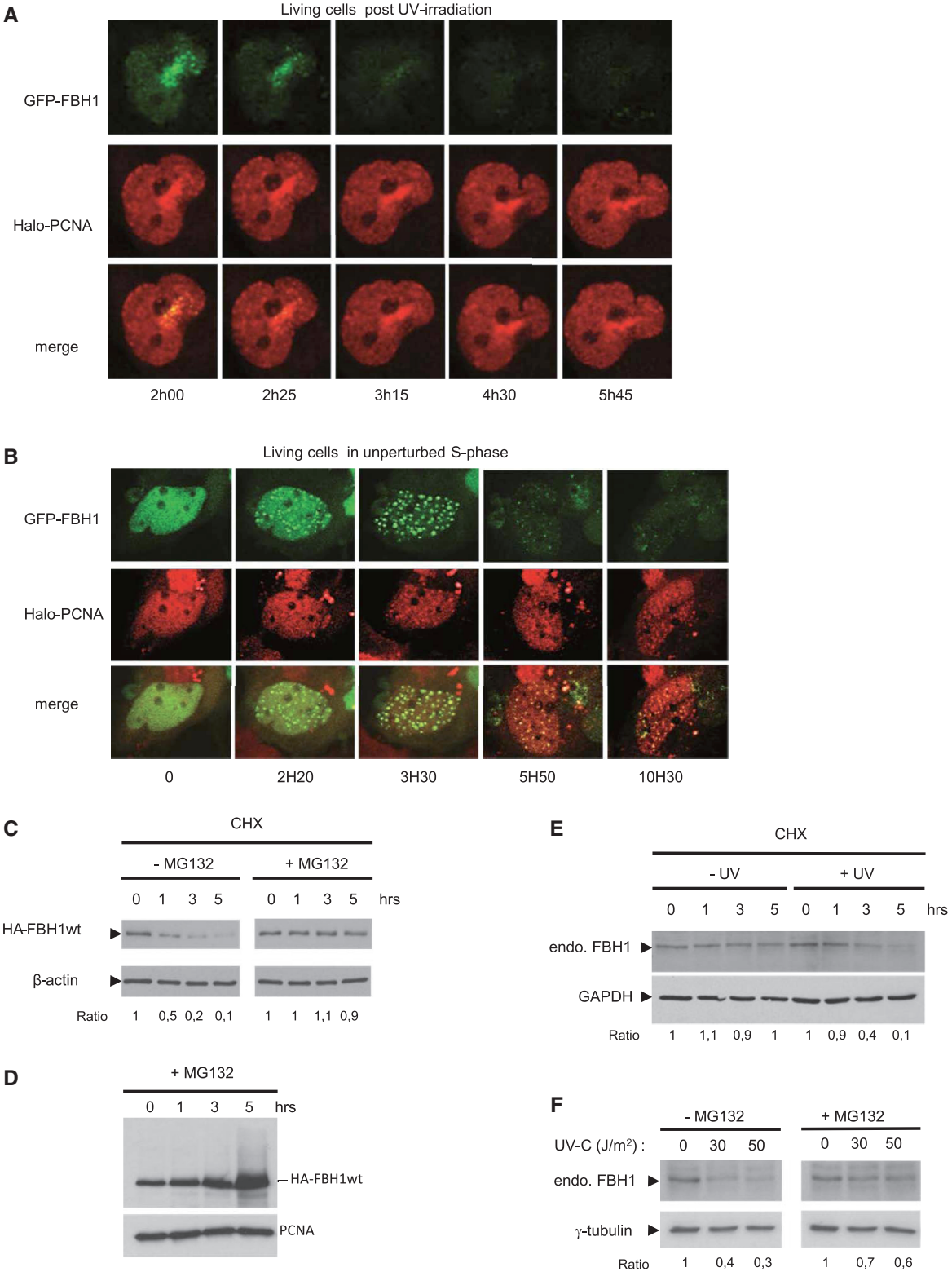

Figure 3. FBH1 is unstable at DNA replication sites or upon UV irradiation. (**A**) MRC5 cells stably expressing Halo-PCNA were transfected with GFP-FBH1. After staining of Halo-PCNA with TMR ligand, cells were locally irradiated then live cells imaged 1.30 h later. Representative distributions of GFP-FBH1 and PCNA are shown at indicated time. (**B**) As in (A) in non-irradiated S-phase cells. (**C**) MRC5 cells expressing HA-FBH1 were treated with cycloheximide (CHX) with or without MG132. Protein levels of HA-FBH1 were monitored by immunoblotting with anti-HA antibody. β-actin shows equal protein loading. Ratio of HA-FBH1 to β-actin levels is presented for each time-point with value arbitrary fixed to 1 for time 0 h. (**D**) Slower migrating bands detected by immunoblotting with FBH1 antibody from cells expressing HA-FBH1wt and treated with MG132 for indicated time. (**E**) HeLa cells were irradiated or not at 50 J/m^2 then incubated with CHX. Protein levels of FBH1 and GAPDH were monitored with specific antibodies. (**F**) HeLa cells were irradiated with UV-C doses ranging from 0 to 50 J/m^2 and subsequently incubated or not in MG132. Levels of FBH1 and γ-tubulin were monitored with specific antibodies. Ratio of FBH1 to γ-tubulin levels is presented. The experiments displayed in (C), (E) and (F) were performed at least three times, and each blot shows representative result.

cells. In contrast to overexpressed FBH1 in MRC5 cells, we were unable to detect a decrease of endogenous FBH1 level in the absence of exogenous DNA damage in HeLa cells. In contrast, we observed a massive reduction of the FBH1 half-life after UV irradiation (Figure 3E). Moreover, we observed that 4 h post-irradiation, endogenous FBH1 levels were inversely related to increasing doses of UV, and these decreases were prevented by addition of MG132 (Figure 3F). Intriguingly, we noticed that early after irradiation, endogenous FBH1 levels remain rather stable, contrary to Cdt1, which is also degraded by the proteasome in response to UV irradiation (23). FBH1 became unstable only within 3–5 h, due to proteasome-mediated degradation (Supplementary Figure S2E). Taken together, these data revealed that FBH1 protein levels are tightly regulated by the proteasome, and its degradation is enhanced in response to DNA damage.

PCNA and CRL4^{Cdt2} ubiquitin ligase promote FBH1 degradation by the proteasome *via* FBH1 PIP degron

Recent studies revealed that the E3 ligase CRL4^{Cdt2} promotes the ubiquitin-dependent degradation of PCNA-bound proteins following UV irradiation through recognition of a specialized PIP-box named PIP degron (23). This PIP degron mediates the recruitment of Cdt2 through a basic residue four amino acids downstream of the PIP-box, while a threonine and an aspartic acid (TD) at position 5 and 6 confer high affinity to chromatin-bound PCNA. Interestingly, FBH1 PIP-box displays a basic residue at +4, but not the TD motif (Figure 4A). To test whether the CRL4^{Cdt2}–PCNA pathway could be involved in the regulation of FBH1 stability *via* its putative PIP degron, we reduced the expression of the CRL4^{Cdt2} complex by siRNA in MRC5 cell populations stably expressing wild-type HA-FBH1 (Figure 4B). The knock-down of DDB1, Cul4 and PCNA increased the stability of Cdt1, whereas the effect of Cdt2 knock-down was negligible in the absence of genotoxic treatment. Interestingly, CRL4^{Cdt2}–PCNA knock-down also resulted in wild-type FBH1 stabilization. These data suggest that CRL4^{Cdt2} and PCNA modulate FBH1 stability through its PIP degron. In agreement with these results, we found that (i) FBH1 was stabilized independently of the CRL4^{Cdt2}–PCNA knock-down when it was mutated in PIP motif (FBH1 PIPdeg6A) (Figure 4B), and (ii) Cdt2 interacts more strongly with the wt than the PIP degron mutant FBH1 (Supplementary Figures S3A and B). Furthermore, Ni^{2+} pull-down in 293 T cells overexpressing FBH1 and His-ubiquitin (His-Ub) showed that the wild-type FBH1 is efficiently poly-ubiquitinated after MG132 treatment while the level of poly-ubiquitination for the PIP-degron mutant (PIPdeg3A) is reduced (Figure 4C, lanes 4 and 8). These results suggest that the ubiquitination and degradation of FBH1 are dependent of its PIP degron, although we cannot completely rule out the possibility that FBH1 poly-ubiquitination is restricted to the overexpressed proteins. We next asked whether CRL4^{Cdt2} was involved in UV-induced degradation of FBH1 by investigating HA-FBH1 protein levels after UV irradiation, in presence of cycloheximide (Figure 4D). When cells were transfected with non-specific siRNA, wild-type HA-FBH1 levels greatly decreased after UV irradiation. In contrast, the knock-down of Cdt2 alleviated UV-induced FBH1 degradation, very similarly to Cdt1. To demonstrate that CRL4^{Cdt2} also targeted FBH1 PIP degron in response to UV-damage, we examined the effect of UV irradiation on the levels of chromatin-bound FBH1. While the level of wild-type FBH1 decreased after UV irradiation, mutations in PIP degron greatly reduce the UV-induced degradation of FBH1 (Figure 4E). Altogether, our results strongly suggest that FBH1 is ubiquitinated and degraded in a PCNA-Cdt2- and non canonical PIP degron-dependent manner, and this degradation is enhanced after UV irradiation.

Forced expression of FBH1 or failure to degrade FBH1 *via* CRL4^{Cdt2}–PCNA pathway impairs Polη recruitment on chromatin upon UV irradiation

We wished to understand why FBH1 is down-regulated after UV irradiation. It is well documented that UV-induced DNA damage blocks replication fork progression during DNA synthesis and induces the mono-ubiquitination of PCNA. The TLS polymerase Polη specifically binds to mono-ubiquitinated PCNA *via* both its PCNA-binding and ubiquitin-binding motifs to facilitate the bypass of blocking lesions thereby rescuing DNA replication and preventing replication fork collapse (14,24). Given the critical role of Polη during translesion DNA synthesis (TLS) and its common partner with FBH1 i.e. PCNA, we tested whether forced FBH1 expression could compete with Polη for PCNA-induced recruitment to damaged DNA. For that, we examined the impact of HA-FBH1 overexpression on the localization of GFP-Polη into UV-induced replication foci (Figure 5A and B). It has previously been demonstrated that GFP-Polη complements XP-V cells indicating that the GFP tag does not affect the biological function of Polη (20).When cells were co-transfected with the HA vector alone, 60% of them displayed Polη foci 3 h after UV irradiation. Strikingly, expression of HA-FBH1 at high levels significantly interfered with the recruitment of Polη into UV-induced nuclear foci (Figure 5A and B). Single mutation in PIP-box or APIM partially restores Polη recruitment, whereas the double mutant fully restores it (Figure 5A and B).

To rule out the possibility that the inhibitory effect of FBH1 on Polη recruitment could be due to a decreased PCNA mono-ubiquitination, we analysed the impact of high levels of HA-FBH1 on both GFP-Polη and mono-ubiquitinated PCNA binding to the chromatin after UV irradiation (Figure 5C). As expected, when co-expressed with HA, Polη recruitment to the chromatin (Chr) increased 3 and 6 h after UV irradiation, together with mono-ubiquitinated PCNA. In agreement with the Figure 5B, we found that exogenous wt HA-FBH1 reduced the binding of Polη to the chromatin, especially 3 h post-UV while the mutant, which is unable to bind PCNA, has no impact on Polη recruitment. These results

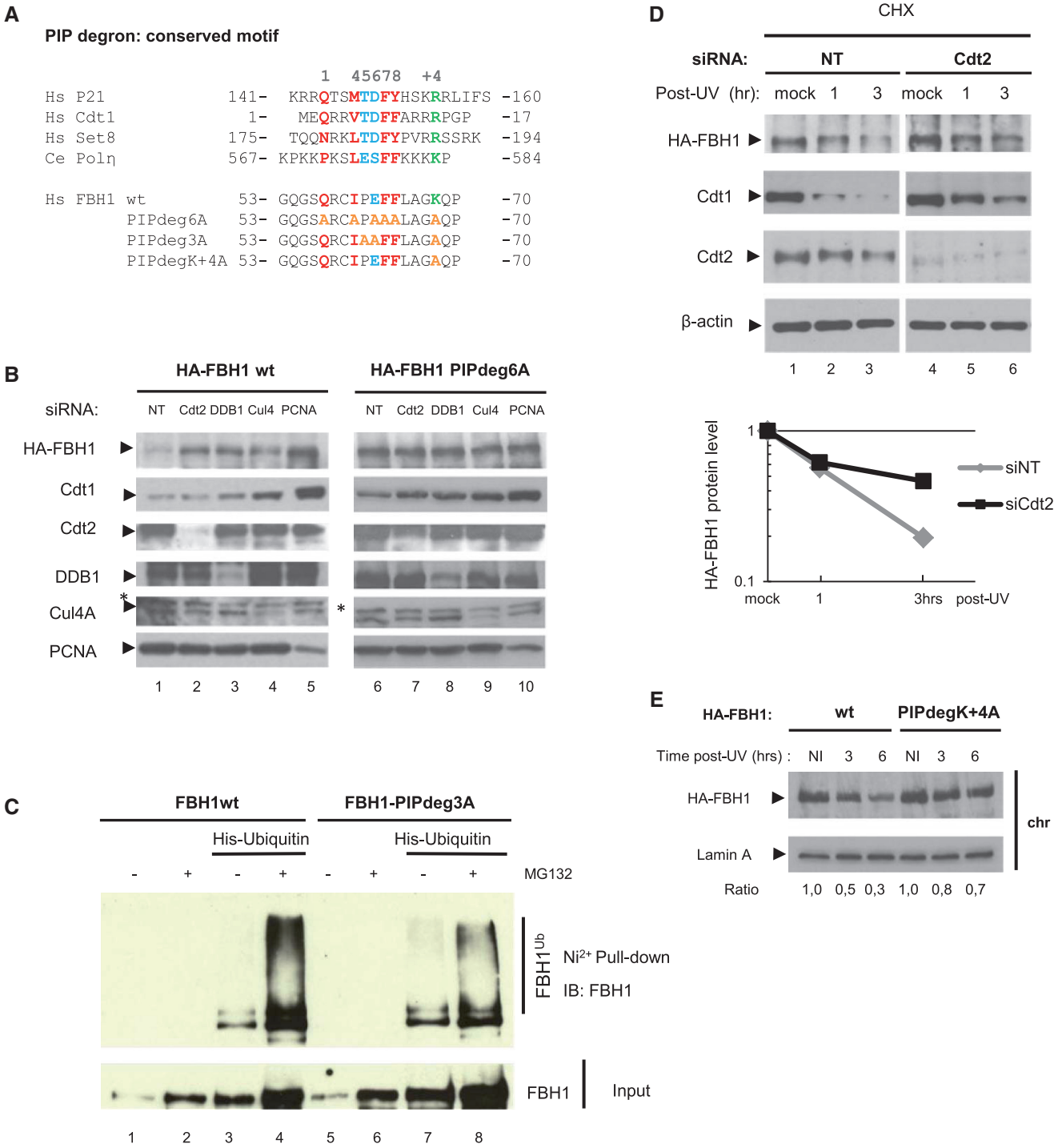

Figure 4. FBH1 is targeted by CRL4-Cdt2 and PCNA for degradation via a non-canonical PIP degron. (**A**) Alignment of PIP degron containing proteins and putative PIP degron of FBH1. Canonical PIP residues (red), 'Degron-specific' basic residue at +4 (green) and 'TD motif' (blue) are figured, with mutant sequences used in this study. (**B**) MRC5 cells stably expressing HA-FBH1 wt or a PIP degron mutant (PIPdeg6A) were transfected with non-targeted siRNA (NT) or siRNAs targeting Cdt2, DDB1, Cul4A and B, or PCNA. Levels of HA-FBH1, Cdt1 and proteins depleted by siRNAs were monitored with specific antibodies. (**C**) 293T cells were transiently co-transfected with wt or a PIP degron mutant (PIPdeg3A) of FBH1, and His-tagged ubiquitin when indicated. Cells were then incubated or not with MG132, and His-ubiquitinated (His-Ub) proteins were Ni^{2+} pulled-down in denaturing conditions. His-Ub FBH1 levels were immunodetected by western blotting with anti-FBH1 antibody. (**D**) MRC5 cells stably expressing HA-FBH1 wt were transfected with non-targeted siRNA (NT) or siRNAs targeting Cdt2. Seventy-two hours later, cells were irradiated or not at 50 J/m^2 and harvested at indicated time. Levels of HA-FBH1, Cdt1 and Cdt2 were monitored with specific antibodies. The blots were quantified using an image reader. (**E**) MRC5 cells transfected with HA-FBH1 wt or HA-FBH1-PIPdegK+4A were irradiated at 50 J/m^2, and FBH1 levels were detected from chromatin fraction (Chr.) at indicated time using HA antibody. Lamin A shows equal protein loading. The experiments displayed in (D) and (E) were carried out at least three times, and each blot shows representative result.

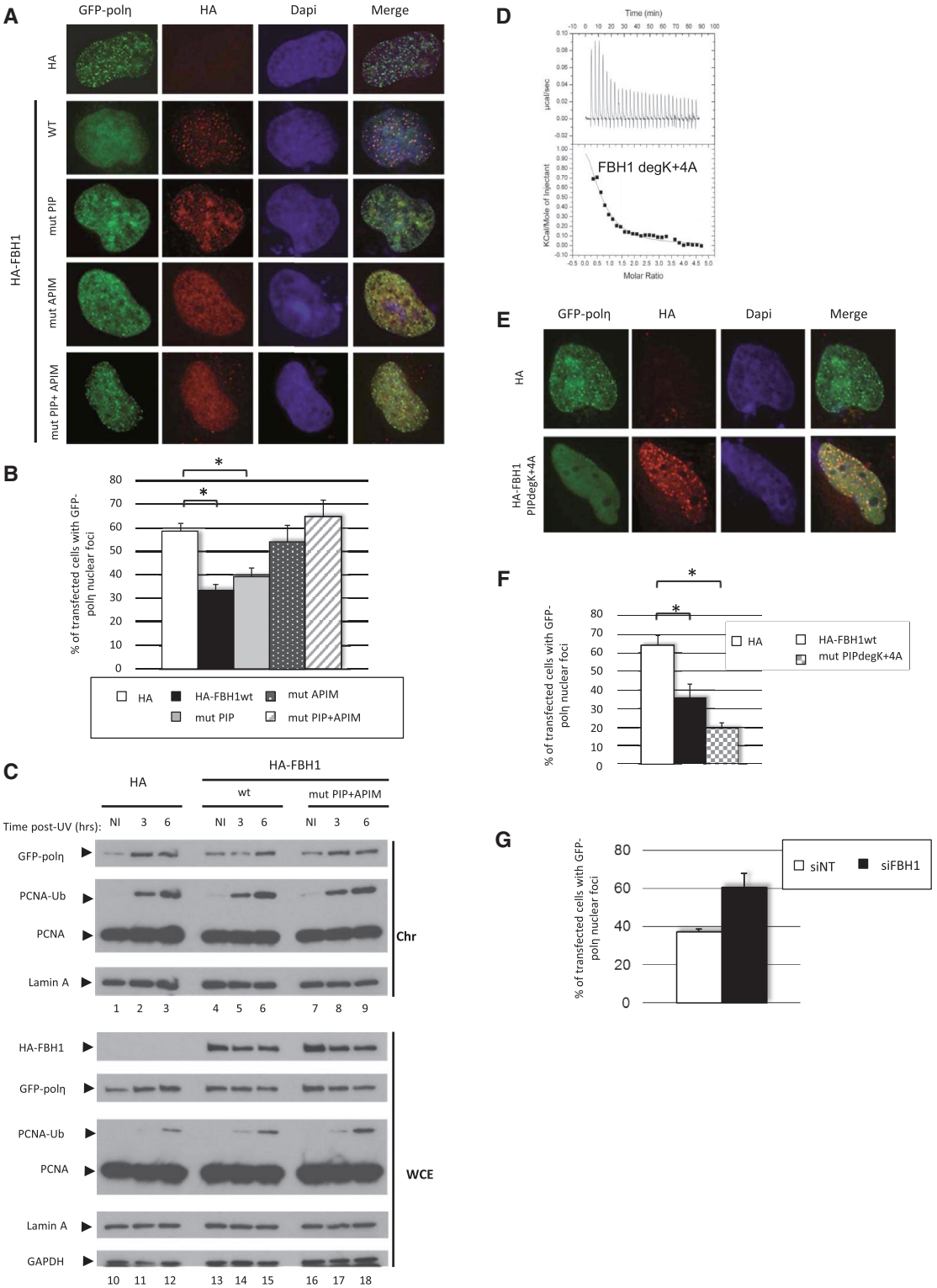

Figure 5. Forced expression of FBH1 or failure to degrade FBH1 via CRL4-Cdt2–PCNA pathway impairs Polη recruitment on chromatin upon UV irradiation. (**A**) MRC5 cells transfected with GFP-polη and indicated HA-FBH1 constructs were UV irradiated at 20 J/m^2. Then 3 h later, the subnuclear localisation of GFP-polη (green) and HA-FBH1 (red) was analysed by immunofluorescence. Representative images are shown. (**B**) The graph shows the percentage of transfected cells displaying Polη foci from experiment described in (A). Mean of three independent experiments (±SD), *$P < 0.05$ by Student's *t*-test. (**C**) MRC5 cells transfected with GFP-polη and either HA, HA-FBH1wt or HA-FBH1 PIP+APIM plasmids, were mock-treated or UV irradiated at 20 J/m^2. Three and six hours later, whole cell extracts (WCE) and insoluble fractions (Chr.) were collected and analysed with indicated antibodies. (**D**) Thermogram and binding isotherm of titration of FBH1 PIP degK+4A peptide into PCNA solution was assessed by ITC at 6°C as described in 'Materials and Methods' section. (**E**) As in (A) with indicated constructs. Representative images are shown. (**F**) The graph shows the percentage of transfected cells displaying Polη foci from experiment described in (E). Mean of three independent experiments (±SD) *$P < 0.05$ by Student's *t*-test. (**G**) MRC5 cells transfected with siRNA (unspecific NT or against FBH1) and GFP-polη were UV irradiated at 20 J/m^2. Then 3 h later, the subnuclear localisation of GFP-polη (green) and PCNA (red) was analysed by immunofluorescence. The graph shows the percentage of transfected cells displaying Polη foci. Mean of three independent experiments (±SD).

prompted us to investigate whether this mis-recruitment of Polη could be further enhanced by inhibiting FBH1 degradation. To assess this, we monitored the effect of a non-degradable FBH1 mutant (PIPdegK + 4A), which is not impaired for its interaction with PCNA and thus localizes into replication foci and UV-induced DNA damage as the wild-type helicase (Table 1, Figures 5D, and data not shown). We found that it inhibited Polη recruitment to a greater extent than the wild-type (Figure 5E and F). Conversely, we observed that the down-regulation of FBH1 using specific siRNA facilitated the Polη foci formation after UV irradiation (Figure 5G). Altogether, this results support the notion that $CRL4^{Cdt2}$–PCNA-dependant degradation of FBH1 is required for Polη proper recruitment to UV lesions.

DISCUSSION

In this study, we have emphasized the importance of PCNA in FBH1 recruitment to sites of replication and DNA damage probably to restrict inappropriate recombination events in human cells. This recruitment is mediated by two motifs: a PIP-box and an APIM motif. More importantly, we discovered that soon after its re-localization, FBH1 is targeted for degradation by the $CRL4^{Cdt2}$–PCNA pathway *via* its PIP degron. Furthermore, forced expression of FBH1 or failure to degrade FBH1 via $CRL4^{Cdt2}$–PCNA pathway impairs Polη recruitment on chromatin following UV irradiation. Collectively, our findings highlighted a subtle way to regulate translesion synthesis, at the expense of homologous recombination, during the S-phase of the cell cycle and after genotoxic stress in human cells.

Interaction between FBH1 and PCNA: characteristics of the APIM and PIP motifs

We have identified two PCNA-interacting motifs in FBH1 (a classical PIP-box and an APIM motif) and demonstrated that they mediate the recruitment of FBH1 to sites of replication and DNA damage. Individual mutation of each motif severely affects the re-localization of FBH1, whereas mutations on both motifs completely abrogate its recruitment. The thermodynamic study of APIM binding to PCNA also shows for the first time that this motif binds directly to PCNA. In addition, competition experiments between p21 PIP-box and FBH1 APIM demonstrate that both motifs bind to the same region of PCNA, i.e. the interdomain connecting loop (IDCL), or at least to close subdomains (Supplementary Figure S1D). Given the fact that the PIP-box and the APIM motif do not compensate for each other loss *in vivo*, our data suggest that they act cooperatively in mediating FBH1 recruitment. In line with this, PIP and APIM motifs are positioned at each terminus of FBH1 amino acids sequence. Because the homotrimeric structure of PCNA enables the binding of three different peptides to PCNA IDCL, we hypothesize that FBH1 may robustly interact with two PCNA monomers *via* its PIP and APIM motifs (Supplementary Figure S5). Crystallographic study of FBH1 binding to PCNA is required to investigate this hypothesis and define more precisely the binding region of the APIM motif.

FBH1 as a novel target for PCNA–$CRL4^{Cdt2}$ degradation pathway

We have revealed that the levels of FBH1 protein are regulated at least by the $CRL4^{Cdt2}$ E3 ubiquitin ligase, which promotes the degradation of FBH1, especially after UV irradiation. As mentioned above, $CRL4^{Cdt2}$ substrates display a specialized PIP-box named PIP degron, which usually contains two important elements: residues TD at position 5 and 6 in the PIP-box that confer high affinity binding to chromatin-bound PCNA and a positively charged residue, at +4 from the PIP-box, which is required for the recruitment of Cdt2. While this latter critical residue is present in FBH1 protein, the TD motif is not conserved (PE instead of TD). However, the high affinity binding with PCNA could be strengthened by the APIM motif. Interestingly, a FBH1 mutant deficient in PIP degron (FBH1-PIPdeg3A) is less efficiently ubiquitinated than wild-type FBH1 (Figure 4C) in non-irradiated cells demonstrating that this motif is critical for the *in vivo* ubiquitination of FBH1.

However, PIP degron-independent polyubiquitination and degradation of FBH1 is still detected (Figure 4C and E), suggesting that an additional pathway regulates FBH1 stability. Indeed, we and others have observed that the mutation of FBH1 F-box motif, which is involved in the formation of an SCF ubiquitin ligase complex, increases the stability of the helicase [(5), and data not shown], suggesting that FBH1 could also be auto-regulated via its F-box.

FBH1 as a 'molecular switch' to prevent HR events and promote TLS pathway in human cells?

Our results show that PCNA has a dual role in FBH1 regulation: it both mediates its recruitment to DNA damage and replication foci, and coordinates its destruction. In contrast to most $CRL4^{Cdt2}$ substrates, including p21, Cdt1 and Set8 (25), FBH1 is not rapidly degraded upon S-phase entry or after UV-induced DNA damage. Indeed, we observed that soon after UV irradiation (<3 h), FBH1 remains stable and accumulates at sites of DNA damage, while 3 to 5 h post-UV, FBH1 is degraded in PCNA–$CRL4^{Cdt2}$-dependent manner. This temporal regulation seems to indicate a mode of 'action/degradation' of FBH1 in human cells after DNA damage. It was previously suggested that FBH1 acts as an anti-recombinase by displacing Rad51 from chromatin (6) and its *S. pombe* orthologue inhibits Rad51-dependent recombination at replication forks (9). Our study suggests that the anti-recombinogenic role of FBH1 partially depends on its interaction with PCNA through the PIP-box and the APIM motif. Altogether, these results imply a novel PCNA-dependent regulation pathway for HR in human cells, in which PCNA recruits an anti-recombinase and subsequently promotes its degradation.

The role of PCNA in HR regulation is well documented in yeast *S. cerevisiae* (26). yPCNA can be modified by the small ubiquitin-like modifier SUMO during unperturbed

S-phase or in response to a lethal dose of DNA damage. This PCNA modification promotes the recruitment of the anti-recombinase Srs2, which disrupts Rad51 nucleoprotein filaments limiting the unscheduled recombination events (4,10,11). Therefore, SUMO–PCNA has an inhibitory effect on HR in budding yeast. In higher eukaryotes, the role of PCNA in HR regulation remains to be clarified. Numerous helicases that are implicated in HR regulation, including Wrn and Blm, interact with PCNA. Very recently, the PCNA-interacting protein PARI has been shown to restrict HR events by interfering with Rad51 (27). In addition, PARI is able to bind SUMO–PCNA *in vitro*, suggesting that it can modulate the recombination events in human cells. However, the question of the regulation of PARI's activity along the cell cycle and in response to DNA damage was not fully addressed.

In this article, we provide evidence for a PCNA-dependant temporal regulation of the helicase FBH1 in human cells. It will be of high interest to further investigate how these different PCNA-interacting helicases are coordinated in human cells to limit inappropriate HR events.

Very recently, two different studies have shown that FBH1 induces DNA double-strand breaks and apoptosis in response to replication stress (28,29). During this process, FBH1 helicase activity is required for DNA–PK-dependent phosphorylation of RPA2 on Serine 4 and 8 while its PIP-box motif is not necessary (29), partly ruling out the role PCNA-dependent recruitment has in this new aspect of FBH1 function in mammalian cells. Because the role of the APIM motif was not addressed, it would be of interest to investigate whether this PCNA interacting motif is required in FBH1-induced double-strand breakage and cell death.

What could be the biological relevance of UV-induced FBH1 degradation?

We have found that the degradation of FBH1 is required to enable efficient recruitment of Polη to chromatin after UV irradiation. Indeed, forced expression of FBH1 impairs the formation of UV-induced Polη foci. This effect is even more severe when FBH1 cannot be degraded by the $CRL4^{Cdt2}$ pathway. This competitive relationship between Polη and a PIP degron containing protein was previously described for p21 (30). The inhibitory effect of FBH1 depends on its PCNA-interacting motifs (PIP and APIM), indicating that FBH1 should compete with Polη for PCNA binding. Following UV irradiation, Polη directly interacts with mono-ubiquitinated PCNA *via* its non canonical PIP-box and a Ubiquitin-Binding Domain (UBZ) (14,24). Given the affinity of FBH1 to PCNA, we assume that in response to UV, its degradation is critical for optimal recruitment of Polη and efficient bypass at stalled replication forks.

In conclusion, our data together with previous studies put forward the position of PCNA at the crossroads of HR and TLS pathways in mammalian cells. In our model, we propose that PCNA first restricts HR through the recruitment of FBH1 to sites of replication and DNA damage. Afterward, PCNA would stimulate TLS *via* the destruction of FBH1 and subsequent recruitment of Polη (Supplementary Figure S5). It is noteworthy that $CRL4^{cdt2}$ could simultaneously degrade FBH1 and facilitate the mono-ubiquitination of PCNA (31), which in turn would promote the recruitment of Polη.

SUPPLEMENTARY DATA

Supplementary Data are available at NAR Online: Supplementary Figures 1–5 and Supplementary Movies 1–4.

ACKNOWLEDGEMENTS

We are grateful to C. Gelot and S. Aoufouchi (IGR, France) for providing Halo-tagged PCNA and His-tagged ubiquitin plasmids and José Cébrian (IGR, France) for providing stable cell population expressing Halo-tagged PCNA. We thank members of the Kannouche lab for helpful discussions.

FUNDING

Ministère de l'Enseignement Supérieur et de la Recherche and the Association pour la Recherche sur le Cancer [DOC20110603022 to A.B.]. Funding for open access charge: La Ligue Nationale contre le Cancer (Equipe labellisée) (to P.L.K. lab); Institut National du Cancer [2010-1-PLBIO-08]; Agence Nationale de la Recherche [ANR-09-PIRI-001].

Conflict of interest statement. None declared.

REFERENCES

1. Li,X. and Heyer,W.D. (2008) Homologous recombination in DNA repair and DNA damage tolerance. *Cell Res.*, **18**, 99–113.
2. Branzei,D. and Foiani,M. (2007) RecQ helicases queuing with Srs2 to disrupt Rad51 filaments and suppress recombination. *Genes Dev.*, **21**, 3019–3026.
3. Krejci,L., Van Komen,S., Li,Y., Villemain,J., Reddy,M.S., Klein,H., Ellenberger,T. and Sung,P. (2003) DNA helicase Srs2 disrupts the Rad51 presynaptic filament. *Nature*, **423**, 305–309.
4. Veaute,X., Jeusset,J., Soustelle,C., Kowalczykowski,S.C., Le Cam,E. and Fabre,F. (2003) The Srs2 helicase prevents recombination by disrupting Rad51 nucleoprotein filaments. *Nature*, **423**, 309–312.
5. Chiolo,I., Saponaro,M., Baryshnikova,A., Kim,J.H., Seo,Y.S. and Liberi,G. (2007) The human F-Box DNA helicase FBH1 faces Saccharomyces cerevisiae Srs2 and postreplication repair pathway roles. *Mol. Cell. Biol.*, **27**, 7439–7450.
6. Fugger,K., Mistrik,M., Danielsen,J.R., Dinant,C., Falck,J., Bartek,J., Lukas,J. and Mailand,N. (2009) Human Fbh1 helicase contributes to genome maintenance via pro- and anti-recombinase activities. *J. Cell Biol.*, **186**, 655–663.
7. Kim,J.H., Kim,J., Kim,D.H., Ryu,G.H., Bae,S.H. and Seo,Y.S. (2004) SCFhFBH1 can act as helicase and E3 ubiquitin ligase. *Nucleic Acids Res.*, **32**, 2287–2297.
8. Kohzaki,M., Hatanaka,A., Sonoda,E., Yamazoe,M., Kikuchi,K., Vu Trung,N., Szuts,D., Sale,J.E., Shinagawa,H., Watanabe,M. *et al.* (2007) Cooperative roles of vertebrate Fbh1 and Blm DNA helicases in avoidance of crossovers during recombination initiated by replication fork collapse. *Mol. Cell. Biol.*, **27**, 2812–2820.
9. Lorenz,A., Osman,F., Folkyte,V., Sofueva,S. and Whitby,M.C. (2009) Fbh1 limits Rad51-dependent recombination at blocked replication forks. *Mol. Cell. Biol.*, **29**, 4742–4756.

10. Papouli,E., Chen,S., Davies,A.A., Huttner,D., Krejci,L., Sung,P. and Ulrich,H.D. (2005) Crosstalk between SUMO and ubiquitin on PCNA is mediated by recruitment of the helicase Srs2p. *Mol. Cell*, **19**, 123–133.
11. Pfander,B., Moldovan,G.L., Sacher,M., Hoege,C. and Jentsch,S. (2005) SUMO-modified PCNA recruits Srs2 to prevent recombination during S phase. *Nature*, **436**, 428–433.
12. Armstrong,A.A., Mohideen,F. and Lima,C.D. (2012) Recognition of SUMO-modified PCNA requires tandem receptor motifs in Srs2. *Nature*, **483**, 59–63.
13. Moldovan,G.L., Pfander,B. and Jentsch,S. (2007) PCNA, the maestro of the replication fork. *Cell*, **129**, 665–679.
14. Kannouche,P.L., Wing,J. and Lehmann,A.R. (2004) Interaction of human DNA polymerase eta with monoubiquitinated PCNA: a possible mechanism for the polymerase switch in response to DNA damage. *Mol. Cell*, **14**, 491–500.
15. Watanabe,K., Tateishi,S., Kawasuji,M., Tsurimoto,T., Inoue,H. and Yamaizumi,M. (2004) Rad18 guides poleta to replication stalling sites through physical interaction and PCNA monoubiquitination. *EMBO J.*, **23**, 3886–3896.
16. Gilljam,K.M., Feyzi,E., Aas,P.A., Sousa,M.M., Muller,R., Vagbo,C.B., Catterall,T.C., Liabakk,N.B., Slupphaug,G., Drablos,F. *et al.* (2009) Identification of a novel, widespread, and functionally important PCNA-binding motif. *J. Cell Biol.*, **186**, 645–654.
17. Ciccia,A., Nimonkar,A.V., Hu,Y., Hajdu,I., Achar,Y.J., Izhar,L., Petit,S.A., Adamson,B., Yoon,J.C., Kowalczykowski,S.C. *et al.* (2012) Polyubiquitinated PCNA recruits the ZRANB3 translocase to maintain genomic integrity after replication stress. *Mol. Cell*, **47**, 396–409.
18. Havens,C.G. and Walter,J.C. (2011) Mechanism of CRL4(Cdt2), a PCNA-dependent E3 ubiquitin ligase. *Genes Dev.*, **25**, 1568–1582.
19. Dumay,A., Laulier,C., Bertrand,P., Saintigny,Y., Lebrun,F., Vayssiere,J.L. and Lopez,B.S. (2006) Bax and Bid, two proapoptotic Bcl-2 family members, inhibit homologous recombination, independently of apoptosis regulation. *Oncogene*, **25**, 3196–3205.
20. Kannouche,P., Broughton,B.C., Volker,M., Hanaoka,F., Mullenders,L.H. and Lehmann,A.R. (2001) Domain structure, localization, and function of DNA polymerase eta, defective in xeroderma pigmentosum variant cells. *Genes Dev.*, **15**, 158–172.
21. Zlatanou,A., Despras,E., Braz-Petta,T., Boubakour-Azzouz,I., Pouvelle,C., Stewart,G.S., Nakajima,S., Yasui,A., Ishchenko,A.A. and Kannouche,P.L. (2011) The hMsh2-hMsh6 complex acts in concert with monoubiquitinated PCNA and Pol eta in response to oxidative DNA damage in human cells. *Mol. Cell*, **43**, 649–662.
22. Liberti,S.E., Andersen,S.D., Wang,J., May,A., Miron,S., Perderiset,M., Keijzers,G., Nielsen,F.C., Charbonnier,J.B., Bohr,V.A. *et al.* (2011) Bi-directional routing of DNA mismatch repair protein human exonuclease 1 to replication foci and DNA double strand breaks. *DNA Repair (Amst.)*, **10**, 73–86.
23. Havens,C.G. and Walter,J.C. (2009) Docking of a specialized PIP Box onto chromatin-bound PCNA creates a degron for the ubiquitin ligase CRL4Cdt2. *Mol. Cell*, **35**, 93–104.
24. Bienko,M., Green,C.M., Crosetto,N., Rudolf,F., Zapart,G., Coull,B., Kannouche,P., Wider,G., Peter,M., Lehmann,A.R. *et al.* (2005) Ubiquitin-binding domains in Y-family polymerases regulate translesion synthesis. *Science*, **310**, 1821–1824.
25. Abbas,T. and Dutta,A. (2011) CRL4Cdt2: master coordinator of cell cycle progression and genome stability. *Cell Cycle*, **10**, 241–249.
26. Watts,F.Z. (2006) Sumoylation of PCNA: Wrestling with recombination at stalled replication forks. *DNA Repair (Amst.)*, **5**, 399–403.
27. Moldovan,G.L., Dejsuphong,D., Petalcorin,M.I., Hofmann,K., Takeda,S., Boulton,S.J. and D'Andrea,A.D. (2012) Inhibition of homologous recombination by the PCNA-interacting protein PARI. *Mol. Cell*, **45**, 75–86.
28. Fugger,K., Kit Chu,W., Haahr,P., Nedergaard Kousholt,A., Beck,H., Payne,M.J., Hanada,K., Hickson,I.D. and Storgaard Sorensen,C. (2013) FBH1 co-operates with MUS81 in inducing DNA double-strand breaks and cell death following replication stress. *Nat. Commun.*, **4**, 1423.
29. Jeong,Y.T., Rossi,M., Cermak,L., Saraf,A., Florens,L., Washburn,M.P., Sung,P., Schildkraut,C. and Pagano,M. (2013) FBH1 promotes DNA double-strand breakage and apoptosis in response to DNA replication stress. *J. Cell Biol.*, **200**, 141–149.
30. Soria,G., Speroni,J., Podhajcer,O.L., Prives,C. and Gottifredi,V. (2008) p21 differentially regulates DNA replication and DNA-repair-associated processes after UV irradiation. *J. Cell Sci.*, **121**, 3271–3282.
31. Terai,K., Abbas,T., Jazaeri,A.A. and Dutta,A. (2010) CRL4(Cdt2) E3 ubiquitin ligase monoubiquitinates PCNA to promote translesion DNA synthesis. *Mol. Cell*, **37**, 143–149.